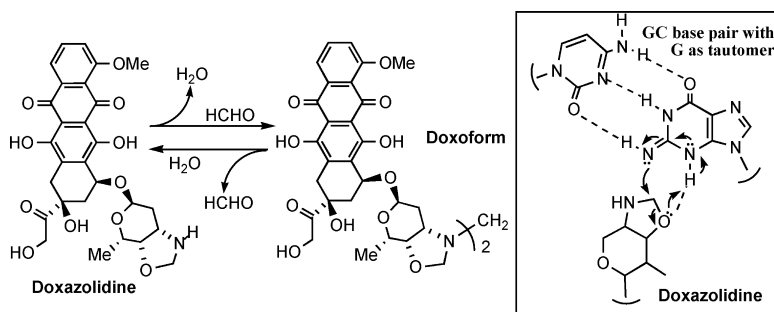


Doxazolidine, a Proposed Active Metabolite of Doxorubicin That Cross-links DNA

Glen C. Post, Benjamin L. Barthel, David J. Burkhart, John R. Hagadorn, and Tad H. Koch
J. Med. Chem., **2005**, 48 (24), 7648-7657 • DOI: 10.1021/jm050678v • Publication Date (Web): 04 November 2005

Downloaded from <http://pubs.acs.org> on March 29, 2009



More About This Article

Additional resources and features associated with this article are available within the HTML version:

- Supporting Information
- Links to the 2 articles that cite this article, as of the time of this article download
- Access to high resolution figures
- Links to articles and content related to this article
- Copyright permission to reproduce figures and/or text from this article

[View the Full Text HTML](#)

Doxazolidine, a Proposed Active Metabolite of Doxorubicin That Cross-links DNA

Glen C. Post,[‡] Benjamin L. Barthel,[‡] David J. Burkhart,[‡] John R. Hagadorn,[‡] and Tad H. Koch^{*,‡,§}

Department of Chemistry and Biochemistry, University of Colorado at Boulder, Boulder, Colorado 80309-0215, and Colorado Cancer Center, Aurora, Colorado 80010

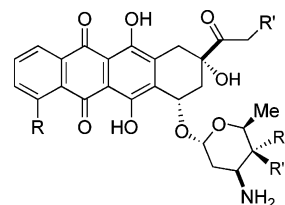
Received July 15, 2005

A crystal structure establishes doxoform as a dimeric formaldehyde conjugate of the oxazolidine of doxorubicin. Doxoform is a prodrug of doxazolidine, a monomeric doxorubicin formaldehyde-oxazolidine. Both doxoform and doxazolidine inhibit the growth of cancer cells at 1–4 orders of magnitude lower concentration than doxorubicin. They also inhibit the growth of cancer cells better than doxsaliform, a prodrug for an acyclic doxorubicin–formaldehyde conjugate. Doxoform rapidly hydrolyzes to doxazolidine, which then hydrolyzes to doxorubicin with a half-life of 3 min in human serum at 37 °C. Both doxoform and doxazolidine are taken up by multidrug-resistant MCF-7/Adr cells 3- to 4-fold better than doxorubicin. A molecular model suggests that doxazolidine can cross-link DNA by direct reaction with a G-base in a tautomeric form with synchronous ring opening of the oxazolidine. These results point to doxoform being a prodrug for doxazolidine that is the reactive species that directly cross-links DNA.

Introduction

Doxorubicin (Dox) is a broad-spectrum antitumor drug of the anthracycline class that has been used in the clinic for more than 30 years for the treatment of leukemias, lymphomas, sarcomas, and solid tumors.¹ Treatment is limited by chronic cardiotoxicity, and extensive research has focused on the mechanism of action toward discovery of methodology to improve the therapeutic index.^{2,3} Many synthetic and natural derivatives have been explored as well as improved drug delivery systems. A stealth liposomal formulation is emerging as a significant improvement.⁴ Shortly after the discovery of Dox, DNA was identified as an important target into which Dox and its clinical congeners, daunorubicin, idarubicin, and epidoxorubicin (Chart 1), reversibly intercalate.^{5,6} Circumstantial evidence accumulating over a period of years from laboratories of Phillips, Konopa, Wang, and Koch, among others, now points to covalent bonding of Dox and its congeners to DNA within the intercalation complex, mediated by formaldehyde.^{7–14} The result is a *virtual cross-linking* of the two strands of DNA by drug, illustrated by the crystal structure in Figure 1. The source of the formaldehyde in vitro and in vivo remains uncertain;¹⁵ however, treatment of MCF-7 breast cancer cells with doxorubicin or daunorubicin results in an intracellular elevation of formaldehyde concentration.¹⁶ These discoveries prompted the syntheses of the doxorubicin–formaldehyde conjugates doxoform (DoxF)¹⁷ and doxsaliform (DoxSF)¹⁸ as drug candidates that carry their own formaldehyde (Scheme 1) and exploration of coadministration of doxorubicin with formaldehyde-releasing prodrugs.^{19,20} For an excellent review of the discovery

Chart 1. Structures for Doxorubicin and Its Clinical Congeners: Epidoxorubicin, Daunorubicin, and Idarubicin



R=OMe, R'=R''=OH, R'''=H: doxorubicin (Dox)
 R=OMe, R'=R''=OH, R'''=H: epidoxorubicin
 R=OMe, R''=OH, R'=R'''=H: daunorubicin
 R''=OH, R'=R'=R''=H: idarubicin

of anthracycline–DNA adducts and virtual cross-links, consult a recent paper by Phillips and co-workers.²¹

DoxF, synthesized by reaction of Dox with formalin, has a dimeric structure with two molecules of Dox condensed with three molecules of formaldehyde (Scheme 1). DoxF is unstable with respect to hydrolysis back to Dox, with a half-life of only a few minutes at 25 °C in RPMI 1640 cell culture medium,¹⁷ but despite this instability, it inhibits the growth of both sensitive and multidrug-resistant tumor cells about equally, with IC₅₀ values ranging from 1 to 4 orders of magnitude lower than those with Dox (Table 1). The magnitude of the difference in efficacy appears to parallel the magnitude of the multidrug resistance. Reaction of DNA with DoxF yields the same cross-links as treatment with Dox and formaldehyde,¹⁷ suggesting that DoxF serves as a prodrug to a monomeric species that cross-links DNA (Scheme 1).

DoxSF is the salicylamide N-Mannich base of Dox with formaldehyde. It releases the acyclic doxorubicin–formaldehyde conjugate with a half-life of 1 h under physiological conditions.¹⁸ The mechanism for cleavage of the N-Mannich base is proposed on the basis of mechanistic studies by London and co-workers²² and our

* To whom correspondence should be addressed at University of Colorado at Boulder. Phone: 303-492-6193. Fax: 303-492-5894. E-mail: tad.koch@colorado.edu.

[‡] University of Colorado at Boulder.

[§] Colorado Cancer Center.

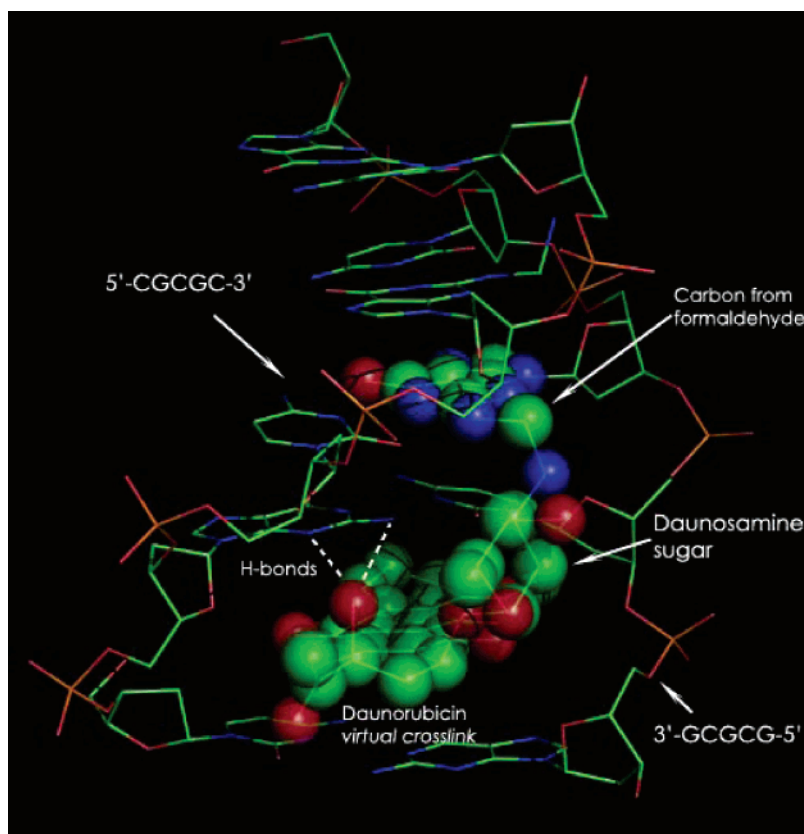


Figure 1. Crystal structure of daunosamine sugar of daunosamine sugar (DoxF) virtually cross-linking double-stranded DNA at 5'-CGC-3'. The daunosamine sugar of daunosamine sugar is in a chair conformation. The virtual cross-linking of the two DNA strands is achieved through a covalent bond to one strand and hydrogen bonding to the other strand plus hydrophobic interactions with both strands. The image was created from data provided by Wang and co-workers¹⁰ at the Rutgers Protein Data Bank (PDB code 1D33) using Chem 3D and PyMOL software.

observation that the cleavage is inhibited at low pH because of protonation at the 3'-amino substituent of DoxSF.¹⁸ The lifetime of the acyclic doxorubicin-formaldehyde conjugate with respect to hydrolysis to Dox is unknown but presumably is very short. DoxSF also inhibits the growth of sensitive and resistant cancer cells at lower concentrations than Dox; however, it is substantially less active than DoxF (Table 1).

We now present evidence that DoxF is a prodrug for monomeric doxorubicin oxazolidine, doxazolidine (Doxaz), and that Doxaz is more reactive than acyclic conjugates in cross-linking DNA. Further, we report the synthesis, isolation, and characterization of Doxaz as well as kinetics for hydrolysis of DoxF to Dox via Doxaz, in vitro activity of Doxaz against sensitive and resistant cancer cells, and a molecular model for reaction of Doxaz with DNA. During the course of these studies we also obtained a crystal structure of DoxF.

Results and Discussion

Synthesis of Doxaz and DoxF. The original syntheses of DoxF and its congeners daunofom and epidofoform (EpiF) were all performed by reaction of the respective clinical drug as its hydrochloride salt with formalin, an aqueous methanolic solution of formaldehyde, in acetate buffer at pH 6. The dimeric conjugates were extracted into chloroform as they were formed. With this method, the presumed intermediate, Doxaz, was not observed. In contrast, reaction of Dox free base in chloroform-*d* solvent with paraformaldehyde, the

polymer of formaldehyde, with monitoring by ¹H NMR showed formation of Doxaz followed by formation of DoxF. Doxaz was isolated 90% pure (73% yield) by stopping the reaction at an intermediate time with the only impurities being traces of Dox and DoxF. Correspondingly, DoxF was isolated in greater than 90% purity (79% yield) by allowing the reaction to continue, again with the only impurity being Doxaz. The structure of Doxaz was established from an intense, doubly charged molecular ion at *m/z* 278.8 in the electrospray mass spectrum and from the high-resolution ¹H NMR data reported in Table 2 with all of the *J* couplings assigned in comparison with data for DoxF. Of particular note in the NMR spectrum of Doxaz is the absence of the singlet peak for the methylene connecting the two oxazolidine rings of DoxF and the characteristic small geminal coupling constant for the methylene protons of the oxazolidine.

The NMR data also partially establish the conformation of the daunosamine sugar of Doxaz and DoxF in chloroform solution as a chair. The proton at the 1'-position is coupled approximately equally to the two protons at the 2'-position in both structures, indicating similar dihedral angles and a chair conformation. Although this is consistent with what others have observed in the crystal structures of various anthracycline antitumor drugs^{23,24} and in the crystal structures of daunosamine sugar (Figure 1) and epidofoform cross-linking DNA,^{10,14} it is not consistent with what we now observe in the crystal structure of DoxF.

Scheme 1. Synthesis of Doxoform (DoxF) and Doxsaliform (DoxSF) from Dox and Their Partial Hydrolysis to Doxazolidine (Doxaz) and Doxorubicin–Formaldehyde Conjugate (Schiff Base or Aminol), Respectively, the Presumed Intermediates for Cross-linking DNA

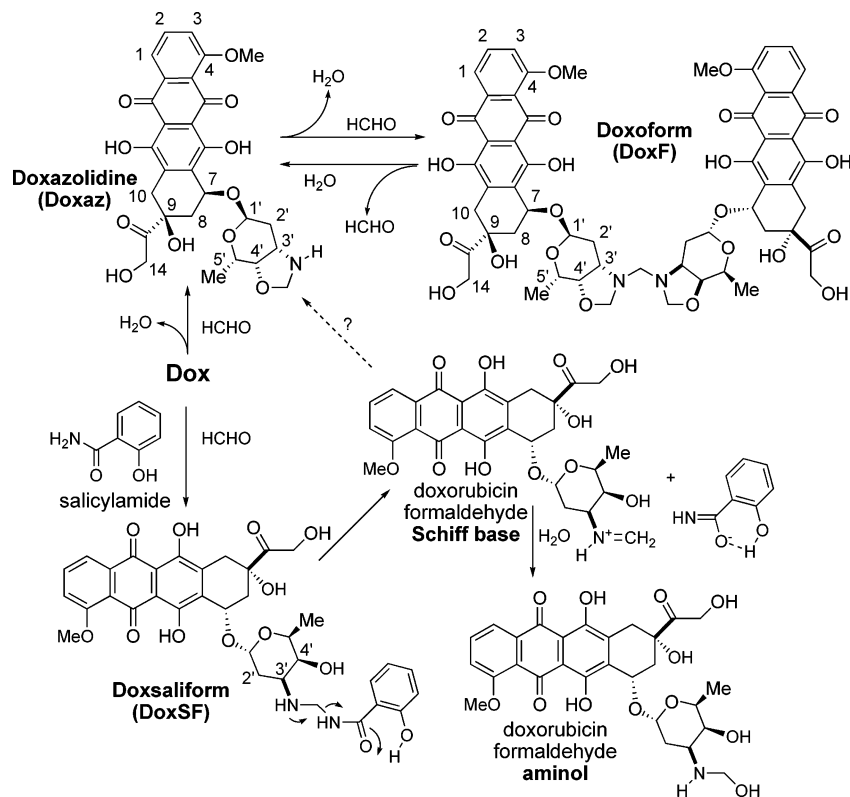


Table 1. Comparison of Growth Inhibition of Breast and Prostate Cancer Cells by Dox, DoxSF, DoxF, Doxaz, Epi, and EpiF^a

compd	IC ₅₀			
	MCF-7	MCF-7/Adr	MDA-MB-435	DU-145
Dox	200 ± 26 ^b	10000 ± 1300 ^b	150 ± 14 ^b	240 ^c
DoxSF	70–80 ^{b,d}	800–2000 ^{b,d,e}	50 ± 9 ^b	
DoxF	2 ^f	1 ^f		3 ^c
Doxaz	3 ± 0.2	3 ± 0.2	7 ± 0.3	4 ± 0.6
Epi	200 ^g	> 10000 ^g		380 ± 52 ^c
EpiF	65 ^g	70 ^g		26 ± 5 ^c

^a Units for IC₅₀ values with Dox, DoxSF, Doxaz, and Epi are nM, and units with DoxF and EpiF are nM equiv to correct for DoxF and EpiF having two active compounds per molecule. IC₅₀ values for Doxaz were determined as described in the Experimental Section. All determinations were done at least in duplicate, with average data shown above. Errors represent 1 standard deviation about the mean for the six wells per lane measured for each drug concentration. ^b Reference 36. ^c Reference 28. ^d Reference 18. ^e Reference 38. ^f Reference 17. ^g Reference 29.

Crystal Structure of DoxF. X-ray quality crystals were grown at the interface of a chloroform solution of DoxF and a mixture of ethyl acetate mixed with hexane. Crystal data and collection parameters appear in Table 3, and a crystallographic information file (CIF format) is provided in Supporting Information. The crystal structure shows a compact structure with the daunosamine sugars in a twist boat conformation and the anthraquinone rings in a π -stacking arrangement shown in Figure 2 together with the crystallographic numbering system. Two least-squares planes were calculated for the groups of six carbon atoms C47–C52 and C19–C24. The two planes are nearly coplanar with a dihedral angle of 0.81(9)°. The atoms from each plane are on average 3.402 Å apart; the individual values vary

little, from 3.37 to 3.44 Å. The crystal structure shows an assortment of intramolecular and four notable intermolecular hydrogen bonds: O6–H6...O12, 2.82 Å; O7–H7...O17, 2.94 Å; O17–H17...O1, 2.84 Å; O18–H18...O6, 3.05 Å. Loss in stability from the twist boat sugar conformations in the solid state with little or no anomeric effect is clearly compensated, partially through π -stacking but probably more importantly through favorable intermolecular interactions including the hydrogen bonds noted.

Cell Experiments. Inhibition of growth of three breast and one prostate cancer cell lines by Dox, DoxSF, DoxF, and Doxaz is compared in Table 1. DoxF and Doxaz inhibit 50% growth at approximately the same concentration for each cell line and inhibit growth at 1 to greater than 3 orders of magnitude lower concentration than Dox. The more dramatic difference occurs with the multidrug-resistant MCF-7/Adr cells that overexpress P-170 glycoprotein efflux pump among other resistance mechanisms.²⁵ The ability of Doxaz to inhibit the growth of MCF-7/Adr cells as well as DoxF is illustrated in Figure 3A, which shows cell growth as a function of drug treatment within a single experiment. All data points fall on the same growth inhibition curve. Growth inhibition parallels drug uptake as measured by flow cytometry measuring drug fluorescence as a function of time after drug treatment. MCF-7/Adr cells take up significantly more DoxF and Doxaz than Dox as shown in Figure 3B. DoxF and Doxaz may be able to overcome P-170 glycoprotein drug efflux pump because unlike Dox they are not cations at physiological pH and consequently are more lipophilic than Dox.²⁶ Further, they are fast-acting drugs in that they can rapidly form

Table 2. ¹H NMR Spectral Assignments for DoxF and Doxaz^a

structure position number																	
1	2	3	4	7	8	9	10	14	Ar-OH	1'	2'	3'	4'	5'	NCH ₂ O	NCH ₂ N	
Doxf																	
7.85	7.69	7.23	3.90	5.10	1.92	4.86	2.86	4.76	12.92	5.48	1.77	3.40	3.98	4.04	4.21	3.52	
dd	dd	dd	OMe	dd	dd	s	d	s	s	dd	ddd	dt	dd	dq	d	s	
(8, 1)	(8, 8.5)	(1, 8.5)	s	(2, 3)	(3, 15)	(OH)	(19)	3.04	13.75	(5, 6)	(5, 6, 15)	(7, 5, 5)	(2, 7)	(2, 6.5)	(4)		
					2.50		3.04	bs	s		2.19				4.73		
					dt		dd	OH			dt				d		
					(15, 2)		(2, 19)				(15, 5, 5)			1.36	(4)		
														Me	(4)		
														q	(6.5)		
Doxaz																	
8.06	7.80	7.41	4.10	5.36	2.16	4.90	3.07	4.78	13.30	5.39	1.70	3.52	3.75	3.96	4.31		
d	t	d	OMe	t	dd	s	d	s	s	dd	ddd	ddd	dd	dq	d		
(8)	(8)	(8)	s	(3)	(3, 15)	(OH)	(19)	3.02	13.97	(6, 7)	(5, 7, 15)	(4, 5, 8)	(2, 8)	(2, 6.5)	(6.5)		
					2.49		3.30	bs	s	s	1.5)			1.34	4.68		
					ddd		dd	OH			2.30			q	d		
					(1.5, 3, 15)		(1.5, 19)				ddd			(6.5)	(6.5)		
											(4, 6, 15)						

^a Spectra were taken at 500 MHz with compounds in DCCl₃. Chemical shifts are in ppm on the δ scale. Coupling constants are in Hz and appear in parentheses. See Scheme 1 for the structures and the number system.

Table 3. Crystallographic Data and Collection Parameters

DoxF	
formula	C ₅₇ H ₅₈ N ₂ O ₂₂
formula wt	1123.05
space group	P3 ₁ (No. 144)
temp (°C)	-119
a (Å)	15.6681(3)
b (Å)	15.6681(3)
c (Å)	17.4559(7)
α (deg)	90
β (deg)	90
γ (deg)	120
Z	3
V (Å ³)	3711.12(18)
d_{calc} (g/cm ³)	1.508
θ range (deg)	1.90–27.87
μ (mm ⁻¹)	0.117
crystal size	0.4 mm × 0.3 mm × 0.2 mm
reflections collected	30332
data/restraints/params	11780/1/730
R1 (for $F_o > 4\sigma F_o$)	0.1071
R1, wR2 (all data)	0.1732, 0.3144
GOF	1.025
largest peak, hole (e/Å ³)	0.48, -0.43

virtual cross-links to DNA such that they are not accessible to the efflux pump. In this respect Figure 3B may underestimate uptake of Doxaz and DoxF because DNA quenches the fluorescence of the Dox chromophore when it cross-links or intercalates DNA.²⁷ Hence, in cells treated with DoxF or Doxaz, a higher percentage of the drug is bound to DNA, which quenches the fluorescence.

DoxSF shows intermediate growth inhibition; of note is the variability in the measurement of the IC₅₀ with MCF-7/Adr cells over numerous measurements by several different co-investigators. Careful scrutiny of the experiments now indicates that DoxF is a byproduct of the synthesis of DoxSF and that higher IC₅₀ values were determined with more highly purified samples of DoxSF. Hence, we conclude that incorporation of formaldehyde in an acyclic structure as in DoxSF yields a much less active drug conjugate.

Interestingly, the formaldehyde conjugate of epidoxorubicin (Epi), epidoxoform (EpiF), is an order of magnitude less active at inhibition of tumor cell growth than is DoxF, even though Epi is only slightly less active than Dox (Table 1).^{28,29} Like DoxF, EpiF has a dimeric structure from reaction of two Epi molecules with three

Table 4. Rate Constant for the Hydrolysis of Doxaz to Dox at 14 °C as a Function of pH

pH	k (min ⁻¹)	$t_{1/2}$ (min)
5.0	0.17 ± 0.01	4
6.1	0.074 ± 0.002	9
7.5	0.0424 ± 0.0002	16
9.0	0.035 ± 0.001	20
10.4	0.038 ± 0.002	18

formaldehyde molecules; however, because of the trans stereochemistry of the vicinal amino alcohol, the structure is bicyclic with seven-membered rings (Scheme 2). It also virtually cross-links DNA, and the crystal structure of the cross-link is very similar to that formed with daunorubicin shown in Figure 1.¹⁴ Upon hydrolysis, EpiF slowly forms a monomeric species with one formaldehyde attached as an aminol (Scheme 2).²⁸ An aminol structure is also proposed for the intermediate from partial hydrolysis of DoxSF (Scheme 1). On this basis, our working hypothesis is that an anthracycline–formaldehyde conjugate that has an oxazolidine ring or releases a derivative with an oxazolidine ring inhibits the growth of tumor cells much better than an anthracycline–formaldehyde conjugate that releases a derivative with the formaldehyde incorporated as an aminol.

Hydrolytic Stability of DoxF and Doxaz. Both DoxF and Doxaz are relatively stable in dry chloroform and dry DMSO over a period of days. In dry DMSO, Doxaz hydrolyzes to Dox at less than 2% per day at ambient temperature. In aqueous medium, DoxF is very hydrolytically unstable with respect to formation of Doxaz, and Doxaz is hydrolytically unstable with respect to formation of Dox. Injection of DoxF on reverse-phase HPLC only shows peaks for Doxaz and Dox. Consequently, HPLC was used to monitor the kinetics of hydrolysis of Doxaz to Dox at 14 °C as a function of pH. Nonlinear least-squares fitting of the data to a first-order rate law gave the rate constants reported in Table 4. The rate constant for hydrolysis at pH 7.5 corresponds to a half-life of 16 min. The hydrolysis was too rapid to measure the rate at 37 °C. Extrapolation using the rough rule that the rate will double for every 10 °C increase in temperature gives an estimation of the half-life at pH 7.4 and 37 °C of 3–4 min. The rate constant increases with decreasing pH except for the transition

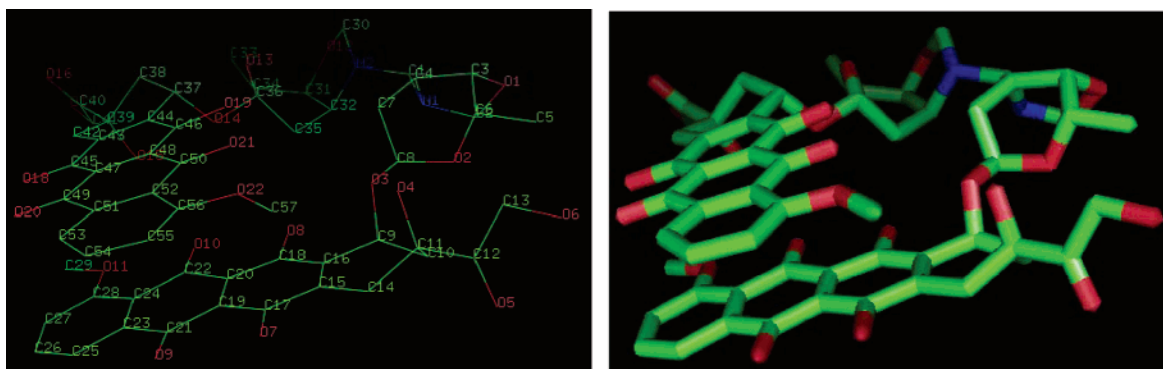


Figure 2. Crystallographic numbering system and three-dimensional structure of DoxF showing twist boat daunosamine sugars and π -stacking arrangement of anthraquinone rings. The image was created in PyMOL from the crystallographic data reported here.

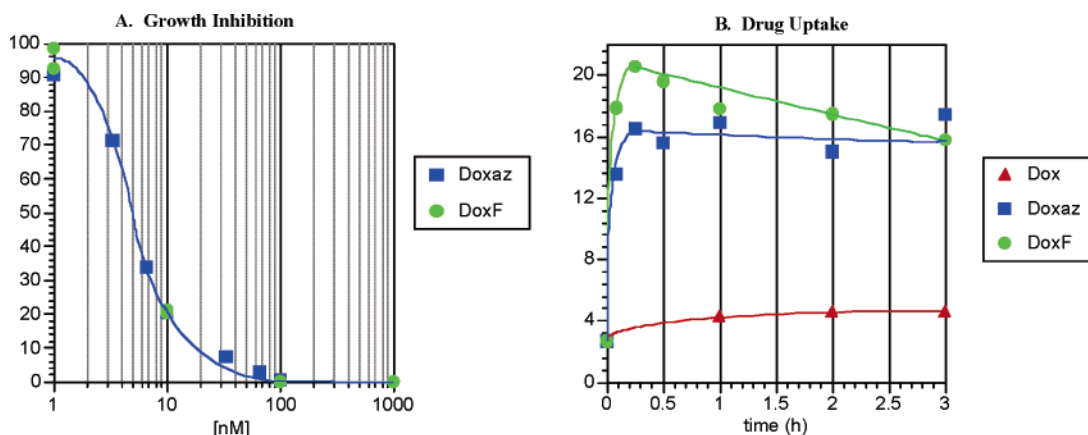
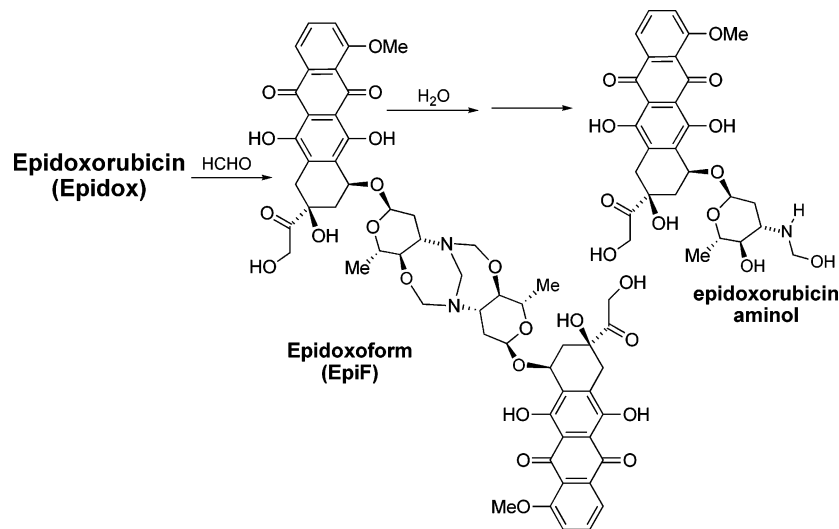


Figure 3. (A) Inhibition of growth of multidrug-resistant MCF-7/Adr breast cancer cells with Doxaz and DoxF as a function of concentration. Cells were treated with drug for 3 h in RPMI 1640 medium containing 10% fetal bovine serum (FBS), and cell growth in the same medium was measured at 5 days. The concentration of DoxF is in nM equiv to correct for DoxF functioning as a prodrug for 2 equiv of Doxaz. (B) Relative fluorescence of the Dox chromophore in MCF-7/Adr cells treated with 500 nM Doxaz, 500 nM equiv of DoxF, or 500 nM Dox as a function of time after inoculation of the cell culture, measured by flow cytometry.

Scheme 2. Synthesis of Epidoxoform (EpiF) from Epidoxrubicin (Epi) and Partial Hydrolysis of EpiF to Epidoxrubicin Aminol, the Presumed Intermediate for Cross-linking of DNA



from pH 10.4 to pH 9.0 where the rate constant decreases slightly. At pH 10.5 the solution appears purple, indicative of deprotonation at one of the hydroquinone functional groups. Hence, at this pH, at least some of the Doxaz has a different charge state. The higher rate at low pH is consistent with acid catalysis, probably assisting hydrolytic ring opening as the slow

step. Which bond of the oxazolidinone ring is broken first, the CH₂-O bond or the CH₂-NH bond, is unknown but may be relevant to a small portion of the biological activity. An intermediate from CH₂-NH bond cleavage would be an unlikely candidate for cross-linking DNA based on the NMR and crystal structures of the virtual cross-link, which all show a diaminomethane linkage

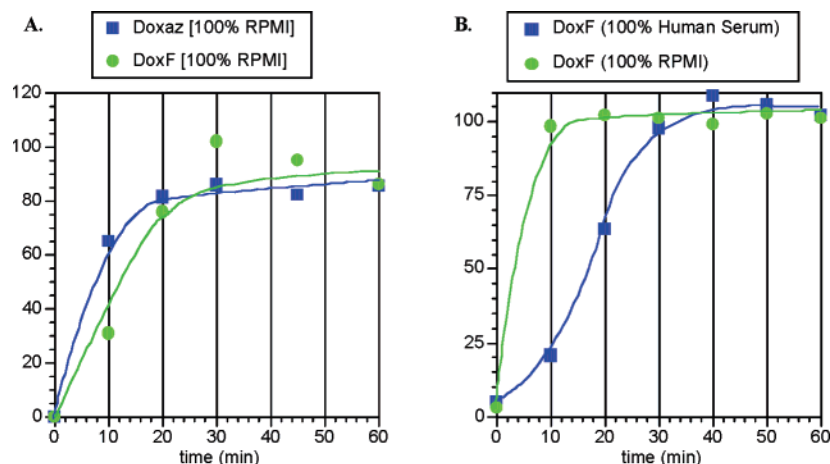


Figure 4. Inhibition of the growth of MCF-7/Adr multidrug-resistant breast cancer cells as a function of time for hydrolysis of Doxaz or DoxF at 37 °C. Cells were treated with drug for 3 h, and cell growth in RPMI 1640 medium containing 10% FBS was measured at 5 days. (A) Starting concentration was 1000 nM equiv of Doxaz or DoxF in RPMI 1640 growth medium. (B) Starting concentration was 100 nM equiv of DoxF in RPMI 1640 growth medium or in 100% pooled human serum.

(Figure 1).^{10,13,14} An intermediate from CH₂-O bond cleavage should be the same reactive intermediate produced by hydrolysis of DoxSF (Scheme 1). With an acid-catalyzed mechanism, CH₂-O bond cleavage would be favored by protonation on oxygen and CH₂-NH bond cleavage would be favored by protonation on nitrogen. This analysis of the ring opening reaction of Doxaz under hydrolytic conditions is relevant to a subsequent discussion of the direct reaction of Doxaz with DNA.

A functional measure of the rate of hydrolysis of Doxaz to Dox (and DoxF to Dox) is the effect of prehydrolysis as a function of time on the growth of MCF-7/Adr cells. This technique provides kinetic information because the concentration of Doxaz at time zero is 1 μM, and at this concentration the product of hydrolysis, Dox, has little activity (Table 1). The result is shown in Figure 4A starting with either Doxaz or DoxF at 1000 nM equiv at 37 °C in RPMI 1640 media and in Figure 4B starting with 100 nM equiv of DoxF in either RPMI 1640 media or in 100% human serum. The media during cell growth was RPMI 1640 containing 10% fetal bovine serum in all the experiments in Figure 4. The data in Figure 4A give an estimate for the half-lives of Doxaz and DoxF at 37 °C in cell culture media. This estimate comes from the IC₅₀ value for cell growth inhibition by Doxaz and DoxF of approximately 2 nM (Table 1) and the requirement of nine hydrolytic half-lives to reach 2 nM Doxaz starting at 1000 nM equiv. Note that after 9 half-lives no DoxF will be present because the rate of hydrolysis of DoxF to Doxaz is much faster than the rate of hydrolysis of Doxaz to Dox. Figure 4A shows 50% growth inhibition by Doxaz after about 8 min for hydrolysis and by DoxF after about 13 min. From these times we estimate the half-life of Doxaz at 8/9 or approximately 1 min and of DoxF at 13/9 or approximately 1.5 min. From the data in Figure 4B, we estimate that human serum extends the half-life of DoxF to about 3 min. For this calculation, 6 half-lives are required to reach 2 nM Doxaz from the starting concentration of 100 nM equiv of DoxF. Human serum may double the life of DoxF through hydrophobic interactions with proteins.

Model for Reaction of Doxaz with DNA. Cell growth inhibition experiments and hydrolysis experi-

ments all point to DoxF serving as a prodrug to Doxaz and Doxaz being the reactive intermediate for virtually cross-linking DNA. Of primary significance is the dramatic difference in cell growth inhibition by Doxaz in comparison with DoxSF. DoxSF releases doxorubicin conjugated to formaldehyde as a Schiff base or aminol (Scheme 1). In principle, Schiff base or aminol could directly cross-link DNA, could cyclize to Doxaz which could cross-link DNA, or could lose formaldehyde to yield Dox. Doxaz could react directly with DNA to create the cross-link or partially hydrolyze to the aminol which could cross-link DNA or lose formaldehyde. In contrast, EpiF can only react with DNA as the aminol because of steric constraints. Further, crystal structures of DNA virtually cross-linked by daunorubicin and epidoxorubicin show very little structural difference,^{10,14} suggesting that the difference in cytotoxicity arises from some factor other than the structure of the cross-link. The data in Table 1 indicate collectively that the oxazolidine inhibits the growth of cancer cells better than the aminol. Is the transition state for direct reaction of the oxazolidine with DNA reasonable? Figure 5 proposes a possibility both schematically and with a molecular model. Whether the reactive intermediate is the oxazolidine or the aminol (or Schiff base), the G-base of the DNA as a HN(2)=C-N(3)H tautomer has the best location of nonbonding electrons and protons for cross-linking without major disruption of Watson-Crick hydrogen bonding. Although formally this tautomerization interconverts double and single bonds, X-ray data on nucleosides bases place the H₂N(2)-C(2) bond only 0.01 Å longer than the C(2)=N(3) bond, which is within experimental error.³⁰ In this tautomeric form, bond breaking and bond forming can occur in concert without development of formal charge. The model suggests that for direct reaction of the oxazolidine, the Doxaz must approach the DNA with the long axis of its anthraquinone approximately parallel to the long axis of the stacked base pairs at the intercalation site. This orientation locates the lone pair of the nucleophilic nitrogen of the cross-linking G-base properly for S_N2 cleavage of the CH₂-O bond of the oxazolidine and locates the oxygen of the oxazolidine near the N-H at the 3-position of the G-base tautomer for proton transfer. After bond forma-

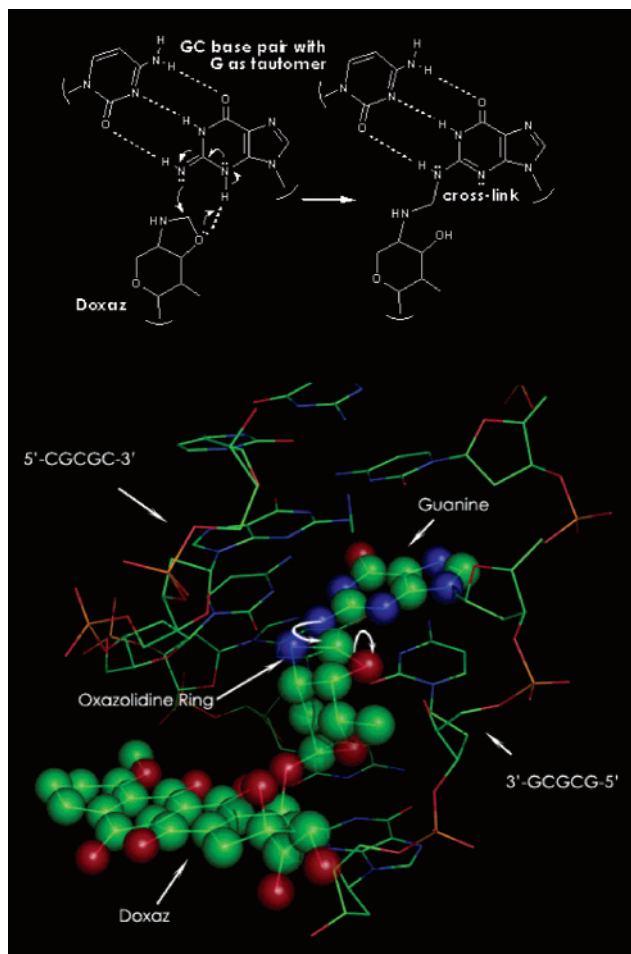
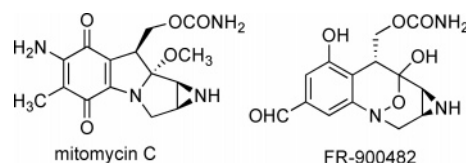


Figure 5. Schematic and molecular model of the reaction of Doxaz with 5'-CGCGC-3'/3'-GCGCG-5' dsDNA to form virtually cross-linked DNA. The model maintains the integrity of electrons in the σ - and π -regions of space, and proceeding through the transition state to product yields no separation of formal charge. The starting point for the molecular model was the structure shown in Figure 1. The daunorubicin was disconnected from the DNA and modified in Chem 3D to create Doxaz. The Doxaz structure was then partially rotated out of the DNA from its fully intercalated position and translated to locate the reactive oxazolidine carbon about 1.6 Å from the reactive nitrogen of the G-base, also in Chem 3D. The final picture is displayed in PyMOL.

tion, bond rotations will allow the anthraquinone to intercalate into the DNA to achieve the virtual cross-link shown in Figure 1.

The proposed mechanism for creation of the covalent bond between Dox–formaldehyde conjugate and the 2-amino group of a G-base (Figure 4) involves a prior tautomerization of the purine at the 2–3 position. This simple in plane proton shift transforms the nitrogen substituent at the 2-position into a nucleophile akin to the nitrogen at the 7-position. The 7-position is the most common site for alkylation in the major groove by the nitrogen mustard, diaziridinylquinone, and cis-platin antitumor drugs.³¹ Other antitumor drugs active in the minor groove that form covalent bonds to the amino group at the 2-position of a G-base include mitomycin C and antibiotic FR-900482 among related structures (Chart 2).³¹ These drugs might also react via the same G-base tautomer. Mitomycin C forms two covalent bonds at the 2-amino groups of the G-bases at 5'-CG-3' sites.³²

Chart 2. Structures for Mitomycin C and FR-900482



Despite the apparent favorability of this tautomer of a G-base for reaction with drugs in the minor groove, it has received little or no attention in the literature probably because detection at low levels is problematic for crystallography or NMR spectroscopy. Further, drugs might induce the tautomerization in a prelude to covalent bonding.

The higher cytotoxicity of DoxF and correspondingly Doxaz might also be explained by DoxF simply serving as a prodrug for Dox that achieves higher Dox levels in cancer cells with virtual cross-linking being only an artifact observed with extracellular DNA. Evidence in support of DNA virtual cross-linking in cancer cells treated with DoxF comes from a labeling experiment reported earlier.³³ MCF-7 and MCF-7/Adr cells were treated with DoxF synthesized with tritiated formaldehyde. After 1 h the cells were lysed and separated into DNA, RNA, and protein fractions, and the fractions were counted for tritium. The ratio of counts in DNA to RNA per milligram of macromolecule was greater than 20 with counts in protein similar to counts in RNA. Control experiments with just tritiated formaldehyde or doxorubicin and tritiated formaldehyde showed a more even distribution of counts in DNA and RNA with a ratio of approximately 2. In control experiments, counts in protein were similar to the experiment with [³H]-DoxF. From this series of experiments, we conclude that DoxF, and now also Doxaz, delivers formaldehyde to DNA in cancer cells. Whether the formaldehyde delivered to cancer cells is actually used with Dox to virtually cross-link DNA is difficult to prove unambiguously, but circumstantial evidence presented here and in earlier papers by our group and other groups points in this direction.

Conclusions

The monooxazolidine derivative of Dox, Doxaz, is synthesized in good yield by the reaction of doxorubicin free base with paraformaldehyde in dry chloroform. Further reaction yields the dimeric compound DoxF, also in good yield. In the solid state, DoxF has π -stacked anthraquinones with daunosamine sugars in a twist boat conformation to achieve a compact structure. In chloroform solution, both DoxF and Doxaz have daunosamine sugars in a relaxed chair conformation. In aqueous medium, DoxF very rapidly hydrolyzes to Doxaz, which relatively rapidly hydrolyzes to Dox. DoxF and Doxaz inhibit the growth of tumor cells approximately equally and significantly better than DoxSF, EpiF, Epi, or Dox despite their rapid hydrolysis to Dox. Of particular significance is the higher activity of Doxaz relative to DoxSF, which is a prodrug for an acyclic Dox–formaldehyde conjugate such as the Schiff base or aminol. Doxaz contains a formaldehyde equivalent in a more stable oxazolidine ring than does Dox aminol or Schiff base. The higher cytotoxicity of Doxaz relative to DoxSF might be explained by the oxazolidine directly

cross-linking DNA without initial ring opening to the Schiff base or aminol. A model for such a direct reaction has the 2-amino of a G-base tautomer attack the oxazolidine ring in an S_N2 reaction. Several strategies for selective delivery of DoxSF to tumor cells show promise in cell experiments.^{34–38} Further, two strategies for delivery of formaldehyde in conjunction with an anthracycline show promise in mouse experiments, one using formaldehyde prodrugs^{19,20,39} and the other using EpiF.⁴⁰ A drug design strategy that protects Doxaz from premature hydrolysis to Dox and delivers Doxaz selectively to tumor cells should dramatically exceed the therapeutic potential of these earlier strategies.

Experimental Section

1. General Remarks. Dox hydrochloride clinical samples (formulated with lactose) were received as a gift from FeRx, Inc. (Aurora, CO). NMR solvents were purchased from Cambridge Isotope Laboratories, Inc. (Andover, MA). All other chemicals were purchased from Aldrich (Milwaukee, WI). Analytical HPLC was performed on a Hewlett-Packard 1090 chromatograph equipped with a diode array UV–vis detector interfaced to an Agilent ChemStation data system (Palo Alto, CA). Analytical HPLC injections were onto an Agilent Zorbax 5 μm reverse-phase octadecylsilyl (ODS) microbore column, 4.6 mm i.d. \times 150 mm, eluting at 1.0 mL/min, and the eluent was monitored at 280 and 480 nm. Analytical separation was achieved using method 1 parameters: flow rate, 1.0 mL/min; eluent A = HPLC grade acetonitrile and eluent B = 20 mM triethylammonium acetate, pH 7.4; gradient, 25:75 A/B at 0 min to 70:30 A/B at 10 min, isocratic to 11 min, back to 25:75 A/B at 13 min. HPLC method 2 parameters were used for monitoring hydrolysis of drugs: flow rate, 1.0 mL/min; eluent A = HPLC grade acetonitrile and eluent B = 20 mM triethylammonium acetate, pH 7.4; gradient, 25:75 A/B at 0 min to 56:44 A/B at 7 min, isocratic to 7.5 min, back to 25:75 A/B at 8.5 min, isocratic to 9 min. ^1H NMR spectra were acquired with a Varian Unity INOVA 500 MHz spectrometer (Palo Alto, CA). Electrospray mass spectra were measured with a Perkin-Elmer Sciex API III instrument (Norwalk, CT), equipped with an ion-spray source, at atmospheric pressure. UV–vis spectrometry was performed with a Hewlett-Packard Agilent 8452A diode array spectrophotometer interfaced to an Agilent ChemStation data system (Palo Alto, CA). The 96-well cell culture plates were read using a PowerWave X plate reader from BIO-TEK Instruments Inc. (Winooski, VT) using their Kenitacal software. Flow cytometry was performed on a Becton Dickinson Biosciences FACScan (San Jose, CA) flow cytometer using Becton Dickinson Biosciences CellQuest Software. All tissue culture materials were obtained from Gibco Life Technologies (Grand Island, NY) unless otherwise noted. MCF-7 human breast adenocarcinoma cells were obtained from American Type Culture Collection (Rockville, MD). MCF-7/Adr, a doxorubicin-resistant subline, was a gift from Dr. William W. Wells (Michigan State University; East Lansing, MI). MDA-MB-435 human breast adenocarcinoma cells were a gift from Drs. Renata Pasqualini and Janet Price (MD Anderson Cancer Center, Houston, TX). DU-145, human, metastatic, prostate, and adenocarcinoma cells were provided by Dr. Andrew Kraft (University of Colorado Health Sciences Center, Denver, CO). MCF-7 and MCF-7/Adr cells were maintained *in vitro* by serial culture in RPMI 1640 medium supplemented with 10% fetal bovine serum, L-glutamine (2 mM), HEPES buffer (10 mM), penicillin (100 units/mL), and streptomycin (100 $\mu\text{g}/\text{mL}$). DU-145 cells were maintained *in vitro* by serial culture in DMEM media with 10% fetal bovine serum. MDA-MB-435 cells were maintained *in vitro* by special culture in DMEM medium supplemented with 5% fetal bovine serum, L-glutamine (2 mM), sodium pyruvate (1 mM), nonessential amino acids and vitamins for minimum essential media, penicillin (100 units/mL), and streptomycin (100 $\mu\text{g}/\text{mL}$). Pooled human serum was obtained from Serologicals

(Norcross, GA). All cells were maintained at 37 °C in a humidified atmosphere of 5% CO_2 and 95% air.

2. Synthesis. 2.1. Doxorubicin Oxazolidine, Doxazolidine (Doxaz). Dox hydrochloride (40 mg, 69 μmol) formulated with lactose (clinical sample) was dissolved in 100 mL of pH 8.5 saturated sodium carbonate/sodium bicarbonate buffer. The aqueous solution was then extracted three times with 250 mL of chloroform. The chloroform extracts were combined, dried over sodium sulfate, and filtered, and the chloroform was removed by rotary evaporation yielding doxorubicin as the free base. Dox free base (30 mg, 55 μmol) was dissolved in 17 mL of deuteriochloroform (3.7 mM) that had been dried over 4 Å molecular sieves for at least 24 h, and the solution was degassed with argon. To this solution, 10 mg of paraformaldehyde (30 wt % of doxorubicin) was added, and the solution was allowed to stir in the dark at ambient temperature (25–28 °C). Progress of the reaction was followed by ^1H NMR, and additional paraformaldehyde (10 mg) was added at 2 and 4 days if further progress was not observed. After 7 days, the reaction was complete as determined by observation of the appearance of oxazolidine doublets at 4.31 and 4.68 ppm and shift of the peak for the 5'-methyl from 1.36 to 1.34 ppm. The reaction mixture was filtered to remove excess paraformaldehyde, and solvent was removed by rotary evaporation to dryness followed by evacuation (\sim 0.05 Torr) for 30 min to give 22 mg of Doxaz (40 μmol , 73% from doxorubicin free base) isolated as a red film. Product was characterized and analyzed for purity by 500 MHz ^1H NMR in chloroform-*d* ($>$ 90% pure, Table 2). Positive ion electrospray mass spectrometry of a solution in THF showed a doubly charged ion at m/z 278.8 ($(M + 2\text{H}^+)/2$, 100% relative intensity, calcd 278.8). HPLC using method 1 shows a peak for Doxaz at 6.6 min (Dox elutes at 4.7 min). HPLC was not reliable for product purity because of some hydrolysis to Dox during elution. The NMR spectrum is provided in Supporting Information.

2.2. Doxoform (DoxF). Dox free base (35 mg 64 μmol) was dissolved in 17 mL of dry chloroform-*d* (3.7 mM), and the solution was degassed with argon. To this solution, 70 mg of paraformaldehyde (200 wt % of doxorubicin) was added, and the solution was allowed to stir in the dark at ambient temperature (25–28 °C). Progress of the reaction was followed by ^1H NMR, which showed the reaction to proceed through the Doxaz intermediate. Additional paraformaldehyde (70 mg) was added after 48 h. After 5 days, reaction was 90% complete as determined by observation of the shift of the peak for the methoxy group from 4.11 to 3.90 ppm. The reaction mixture was filtered to remove excess paraformaldehyde, and the solvent was removed by rotary evaporation to dryness followed by evacuation (\sim 0.05 Torr) for 30 min to give 28 mg (56 μmol , 79%) of DoxF as a red film. Product was analyzed for purity by 500 MHz ^1H NMR in chloroform-*d* ($>$ 90% pure, Table 2). The spectrum is provided in Supporting Information. DoxF is not stable to HPLC, and injections of DoxF only yield peaks for Doxaz and Dox.

3. Crystal Structure of DoxF. 3.1. Growth of DoxF Single Crystals. To synthesize DoxF for growing crystals, 25 mg of Dox hydrochloride (43 mmol) was dissolved in 30 mL of triethylammonium acetate (20 mM)/acetic acid buffer at pH 6.0. Formaldehyde (formalin, 34.9 mL of 37% formaldehyde, 10 M equiv, in aqueous methanol) was added, and the mixture was stirred for 30 min at ambient temperature. Chloroform (100 mL) was added, and the mixture was stirred overnight. The chloroform was then removed with a separatory funnel, and 100 mL of fresh chloroform was added to the aqueous layer. This was allowed to stir until all the color had transferred from the aqueous buffer to the chloroform. The chloroform fractions were combined and dried over sodium sulfate, and the solvent was removed by rotary evaporation. The product was redissolved in a small amount of chloroform and again subjected to rotary evaporation. Three washes with 50 mL aliquots of water were done by swirling the water inside the flask for 1 min. Residual water was removed by evacuation at high vacuum (0.5 Torr). The washed product was dissolved once more in chloroform and collected by removing the solvent.

This product was collected into a clean, dry Eppendorf tube and determined to be sufficiently pure by ^1H NMR. Crystallization of the DoxF was accomplished by placing 10 mg of the crude material inside a 4 mm i.d. glass tube and dissolving it in 0.5 mL of chloroform. This was gently overlaid with 2 mL of 3:1 ethyl acetate/hexane, and the glass tube was sealed to prevent solvent loss. Orange-red block-shaped crystals were formed at the interface between the two solvent systems and were harvested after approximately 1 week.

3.2. X-ray Crystal Structure of DoxF. Crystals of DoxF were suspended in Paratone-N hydrocarbon oil. A single crystal was cut from a cluster, and it was mounted on the tip of a glass fiber and transferred to a Siemens SMART diffractometer/CCD area detector fitted with a low-temperature nitrogen-flow device. The crystal was centered in the beam (Mo K α ; $\lambda = 0.71073$ Å; graphite monochromator). A preliminary orientation matrix and unit cell constants were determined by the collection of 60 10-s frames, followed by spot integration and least-squares refinement. A sphere of data were collected at -119 °C using 0.3° ω scans. The raw data were integrated and the unit cell parameters refined using SAINT. Data analysis was performed using XPREP. Absorption correction was applied using SADABS. The data were corrected for Lorentz and polarization effects, but no correction for crystal decay was applied. Structure solutions and refinements were performed (SHELXTL-Plus V5.0) on F^2 . Table 3 lists a summary of crystal data and collection parameters for DoxF. A crystallographic information file (CIF format) appears in the Supporting Information.

Preliminary data indicated a primitive trigonal cell. Systematic absences and intensity statistics suggested space groups $P3_1$ (No. 144) and $P3_2$ (No. 145). Acceptable solution and refinement in space group $P3_1$ was achieved with stereochemistry consistent with that known for DoxF. Since DoxF is a weak anomalous scatterer, the Flack parameter was poorly defined, but it is near zero ($-0.24(18)$). The inverted structure gave unsatisfactory refinement in $P3_1$ and a Flack parameter approaching unity. All non-H atoms in the model were refined anisotropically. Hydrogens were placed in idealized positions and were included in structure factor calculations but were not refined.

4. DoxF and Doxaz Stability Studies. 4.1. Doxaz Stability in DMSO. Doxaz (22 mg, 40 μmol) was dissolved in 1 mL of DMSO- d_6 (stored over activated 4 Å molecular sieves) and analyzed for purity by 500 MHz ^1H NMR. After a $10\times$ dilution with DMSO to 4 mM, the stability of Doxaz was then followed by HPLC using method 1, observing the relative peak area of the Doxaz peak at 6.6 min with constant injection volume. Doxaz hydrolyzed at a rate of $<2\%$ per day in DMSO.

4.2. Doxaz Stability in Buffers. HPLC buffer, pH 7.4, 20 mM TEAA, was used for the measurement of hydrolysis of Doxaz. The buffer's pH was adjusted as needed with either triethylamine or acetic acid to pH 10.4, 9.0, 6.0, and 5.0 with one sample left unchanged at pH 7.4. A volume of 1950 μL of each of these solutions was added to a conical vial and then cooled to 14 °C. An amount of 50 μL of a 4 mM solution of Doxaz was added to each tube, and hydrolysis was followed by HPLC using method 2 with injections every 10 min. The pH of the buffers was measured before the addition of drug and 1.5 h after the start of hydrolysis. The data were fit to a first-order rate law using regression software from Blackwell Scientific Software (Oxford, U.K.); correction for hydrolysis on the HPLC column was incorporated into the preexponential term of the rate law.

5. Cell Experiments. IC $_{50}$ measurements were performed as follows. Cells were dissociated with trypsin/EDTA, counted, and suspended in growth media to 5×10^3 cells/mL. This cell suspension was dispensed in 200 μL aliquots (1000 cells/well) into the inside wells of 96-well tissue culture plates. Outside wells contained 200 μL of media. Plates were then incubated for 24 h at 37 °C in a humidified atmosphere of 5% CO $_2$ and 95% air. The medium was replaced with 90 μL of growth medium prior to addition of the drug. Doxaz was dissolved in DMSO at concentrations ranging from 50 μM to 1 mM. The

concentration was then corrected by measuring the solution absorbance at 480 nm ($\epsilon = 11\,500\text{ M}^{-1}\text{ cm}^{-1}$). Serial dilutions (1:3 and 1:10) were made in sterile DMSO to yield seven solutions of decreasing drug concentration at $100\times$ the respective working concentrations. The resulting solutions were individually diluted 1:10 in RPMI 1640 medium; 10 μL of the resulting $10\times$ solution was immediately added to the appropriate lane of cells. Additionally, two lanes were treated with 10 μL of growth medium containing 10% sterile DMSO and one lane was treated with 90 μL of 1.5 M Tris-HCl. The cells were incubated at 37 °C for 3 h, at which time the drug solutions were replaced with 200 μL of fresh growth medium. The cells were then incubated for 5 days, and the extent of colony formation was determined using a crystal violet staining assay measuring optical density at 588 and 770 nm.¹⁷

Drug uptake was measured by flow cytometry as follows. Cells were dissociated with trypsin/EDTA, counted, and suspended in growth media to 1×10^5 cells/mL. This cell suspension was dispensed in 2.5 mL aliquots into 6-well tissue culture plates. Plates were then incubated for 24 h at 37 °C in a humidified atmosphere of 5% CO $_2$ and 95% air. The growth media was replaced with 2 mL of fresh growth media prior to addition of the drug. Doxaz, DoxF, and Dox HCl were dissolved in DMSO each at 50 μM . The concentration was then corrected by measuring the solution absorbance at 480 nm ($\epsilon = 11\,500\text{ M}^{-1}\text{ cm}^{-1}$). Drug solution (20 μL) was added to an individual well and was incubated for 5 min, 15 min, 30 min, 1 h, 2 h, or 3 h at 37 °C in a humidified atmosphere of 5% CO $_2$ and 95% air. All drug treatments were performed, so all treatment times would end all at once. After treatment, culture media was removed, cells were washed once with 0.5 mL of HBSS and washed once with 0.5 mL of trypsin/EDTA, 0.5 mL of trypsin/EDTA was added, and cells were incubated for 5 min. After all cells were trypsinized, cells were aspirated with 1.5 mL of cold D-PBS (Dulbecco's phosphate buffered saline, no calcium or magnesium), and this solution was added to 3 mL of cold D-PBS (4.5 mL total D-PBS) in a conical vial. Cells were centrifuged at 200g for 5 min, and D-PBS was decanted off. Cells were washed once more in 5 mL of cold D-PBS and centrifuged at 200g for 5 min, and D-PBS was decanted off. The cells were then aspirated with 1 mL of D-PBS, placed in a sample tube, and kept on ice until needed with FACScan. Cells were analyzed with excitation at 488 nm (15 mW Ar ion laser), with emission monitored between 570 and 600 nm. Instrument settings were optimized for the cell line and held constant for all experiments. For the anthracycline fluorescence analysis, 10 000 cells were analyzed for each sample. The data are presented as the mean fluorescence for each condition.

Hydrolysis of Doxaz or DoxF in RPMI medium was performed as follows. Cells were dissociated with trypsin/EDTA, counted, and suspended in growth media to 5×10^3 cells/mL. This cell suspension was dispensed in 200 μL aliquots (1000 cells/well) into the inside wells of 96-well tissue culture plates. Plates were then incubated for 24 h at 37 °C in a humidified atmosphere of 5% CO $_2$ and 95% air. The medium was replaced with 180 μL of growth medium prior to addition of the drug. RPMI media (no serum added) was divided into 5 mL aliquots in conical vials and heated to 37 °C in a constant-temperature bath. Doxaz and DoxF were dissolved in DMSO at 1 mM equiv. The concentration was then corrected by measuring the solution absorbance at 480 nm ($\epsilon = 11\,500\text{ M}^{-1}\text{ cm}^{-1}$). Drug solution (50 μL) was added to an individual conical vial, and the drug was allowed to hydrolyze (at 10 μM) for 0, 10, 20, 30, 45, 60, 75, or 90 min. Experiments were performed such that all hydrolysis times would end simultaneously. After hydrolysis, 20 μL of the drug solution was added to a lane of wells on the 96-well plate to give a final concentration of 1 μM equiv (sum of Dox and Doxaz and/or DoxF) for treatment of cells. Additionally, two lanes were treated with 20 μL of growth medium containing 1% sterile DMSO for a control. The cells were incubated at 37 °C for 3 h, at which time the drug solutions were replaced with 200 μL of fresh growth media. The cells were then incubated for 5 days, and the extent of

colony formation was determined using a crystal violet staining assay measuring optical density at 588 and 770 nm.

Hydrolysis of DoxF in RPMI medium or 100% human serum was performed the same as above except drug hydrolysis was performed at 1 μ M equiv and drug treatment was at 100 nM equiv. During drug treatment, the medium was either 90% RPMI/10% FBS or 90% RPMI/10% human serum. During cell growth, the medium was 90% RPMI/10% FBS.

Acknowledgment. The authors thank the U.S. Army Prostate Cancer Research Program (Grant No. DAMD17-01-1-0046) and the National Cancer Institute of the NIH (Grant No. CA-92107) for financial support, the National Science Foundation for help with the purchase of NMR equipment (Grant No. CHE-0131003), Dr. William Wells for MCF-7/Adr cells, Drs. Renata Pasqualini and Janet Price for MDA-MB-435 cells, and Dr. Andrew Kraft for DU-145 cells.

Supporting Information Available: Crystallographic information file for DoxF (in CIF format), HPLC data of Doxaz monitored at 280 and 480 nm, and 1 H NMR spectra for Doxaz and DoxF establishing the state of purity. This material is available free of charge via the Internet at <http://pubs.acs.org>.

References

- DeVita, V. T.; Hellman, S.; Rosenberg, S. A. *Cancer: Principles and Practice of Oncology*, 6th ed.; Lippincott, Williams and Wilkins: Philadelphia, PA, 2001.
- Gewirtz, D. A. A critical evaluation of the mechanisms of action proposed for the antitumor effects of the anthracycline antibiotics adriamycin and daunorubicin. *Biochem. Pharmacol.* **1999**, *57*, 727–741.
- Minotti, G.; Menna, P.; Salvatorelli, E.; Cairo, G.; Gianni, L. Anthracyclines: molecular advances and pharmacologic developments in antitumor activity and cardiotoxicity. *Pharmacol. Rev.* **2004**, *56*, 185–229.
- Thigpen, J. T. Innovations in anthracycline therapy: overview. *Community Oncol.* **2005**, *2* (S1), 3–7.
- Arcamone, F. *Doxorubicin Anticancer Antibiotics*; Academic Press: New York, 1981; pp 246–254.
- Chaires, J. B.; Satyanarayana, S.; Suh, D.; Fokt, I.; Przewloka, T.; et al. Parsing the free energy of anthracycline antibiotic binding to DNA. *Biochemistry* **1996**, *35*, 2047–2053.
- Cullinane, C.; van Rosmalen, A.; Phillips, D. R. Does adriamycin induce interstrand cross-links in DNA? *Biochemistry* **1994**, *33*, 4632–4638.
- Cullinane, C.; Cutts, S. M.; van Rosmalen, A.; Phillips, D. R. Formation of adriamycin–DNA adducts in vitro. *Nucleic Acids Res.* **1994**, *22*, 2296–2303.
- Skladanowski, A.; Konopa, J. Interstrand DNA crosslinking induced by anthracyclines in tumour cells. *Biochem. Pharmacol.* **1994**, *47*, 2269–2278.
- Wang, A. H. J.; Gao, Y. G.; Liaw, Y. C.; Li, Y. K. Formaldehyde cross-links daunorubicin and DNA efficiently: HPLC and X-ray diffraction studies. *Biochemistry* **1991**, *30*, 3812–3815.
- Leng, F.; Savkur, R.; Fokt, I.; Przewloka, T.; Priebe, W.; et al. Base specific and regiospecific chemical cross-linking of daunorubicin to DNA. *J. Am. Chem. Soc.* **1996**, *118*, 4731–4738.
- Taatjes, D. J.; Gaudiano, G.; Resing, K.; Koch, T. H. A redox pathway leading to the alkylation of DNA by the anthracycline, anti-tumor drugs, adriamycin and daunomycin. *J. Med. Chem.* **1997**, *40*, 1276–1286.
- Zeman, S. M.; Phillips, D. R.; Crothers, D. M. Characterization of covalent adriamycin–DNA adducts. *Proc. Natl. Acad. Sci. U.S.A.* **1998**, *95*, 11561–11565.
- Podell, E. R.; Harrington, D. J.; Taatjes, D. J.; Koch, T. H. Crystal structure of epidoxorubicin–formaldehyde virtual crosslink of DNA and evidence for its formation in human breast-cancer cells. *Acta Crystallogr.* **1999**, *D55*, 1516–1523.
- Taatjes, D. J.; Gaudiano, G.; Koch, T. H. Production of formaldehyde and DNA–adriamycin or –daunomycin adducts, initiated through redox chemistry of DTT/iron, xanthine oxidase/NADH/iron, or glutathione/iron. *Chem. Res. Toxicol.* **1997**, *10*, 953–961.
- Kato, S.; Burke, P. J.; Fenick, D. J.; Taatjes, D. J.; Bierbaum, V. M.; et al. Mass spectrometric measurement of formaldehyde generated in breast cancer cells upon treatment with anthracycline antitumor drugs. *Chem. Res. Toxicol.* **2000**, *13*, 509–516.
- Fenick, D. J.; Taatjes, D. J.; Koch, T. H. Doxorubicin and daunomycin: Anthracycline–formaldehyde conjugates toxic to resistant tumor cells. *J. Med. Chem.* **1997**, *40*, 2452–2461.
- Cogan, P. S.; Fowler, C. R.; Post, G. C.; Koch, T. H. Doxsaliform: A novel N-Mannich base prodrug of a doxorubicin formaldehyde conjugate. *Lett. Drug Des. Dis.* **2004**, *1*, 247–255.
- Swift, L. P. C.; S. M.; Rephaeli, A.; Nudelman, A.; Phillips, D. R. Activation of adriamycin by the pH-dependent formaldehyde-releasing prodrug hexamethylenetetramine. *Mol. Cancer Ther.* **2003**, *2*, 189–198.
- Nudelman, A.; Levovich, I.; Cutts, S. M.; Phillips, D. R. The role of intracellularly released formaldehyde and butyric acid in the anticancer activity of acyloxyalkyl esters. *J. Med. Chem.* **2005**, *48*, 1042–1054.
- Cutts, S. M.; Nudelman, A.; Rephaeli, A.; Phillips, D. R. The power and potential of doxorubicin–DNA adducts. *IUBMB Life* **2005**, *5*, 73–81.
- Loudon, G. M.; Almond, M. R.; Jacob, J. N. Mechanism of hydrolysis of N-(1-aminoalkyl) amides. *J. Am. Chem. Soc.* **1981**, *103*, 4508–4515.
- Wani, M. C.; Taylor, D. J.; Wall, M. E.; McPhail, A. T.; Onan, K. D. Antitumor agents. XIII. Isolation and absolute configuration of Carminomycin I from *Streptosporangium* sp. *J. Am. Chem. Soc.* **1975**, *97*, 5955–5957.
- Pettit, G. R.; Einck, J. J.; Herald, C. L.; Ode, R. H.; Von Dreele, R. B.; et al. The structure of carminomycin I. *J. Am. Chem. Soc.* **1975**, *97*, 7387–7389.
- Mimnaugh, E. G.; Fairchild, C. R.; Fruehauf, J. P.; Sinha, B. K. Biochemical and pharmacological characterization of MCF-7 drug-sensitive and Adr multidrug-resistant human breast tumor xenografts in athymic mice. *Biochem. Pharmacol.* **1991**, *42*, 391–402.
- Lampidis, T. J.; Kolonias, D.; Podona, T.; Isreal, M.; Safa, A. R.; et al. Circumvention of P-GP MDR as a function of anthracycline lipophilicity and charge. *Biochemistry* **1997**, *36*, 2679–2685.
- Crooke, S. T.; DuVernay, V. H. Fluorescence Quenching of Anthracyclines by Subcellular Fractions. *Anthracyclines Current Status and New Developments*; Academic Press: New York, 1980; pp 151–155.
- Taatjes, D. J.; Fenick, D. J.; Koch, T. H. Epidoxoform: a hydrolytically more stable anthracycline–formaldehyde conjugate, cytotoxic to resistant tumor cells. *J. Med. Chem.* **1998**, *41*, 1306–1314.
- Taatjes, D. J.; Koch, T. H. Growth inhibition, nuclear uptake, and retention of anthracycline–formaldehyde conjugates in prostate cancer cells relative to clinical anthracyclines. *Anti-cancer Res.* **1999**, *19*, 1201–1208.
- Taylor, R.; Kennard, O. The molecular structures of nucleosides and nucleotides. 1. The influence of protonation on the geometries of nucleic constituents. *J. Mol. Struct.* **1982**, *78*, 1–28.
- Rajski, S. R.; Williams, R. M. DNA interstrand cross-linking agents as antitumor drugs. *Chem. Rev.* **1998**, *98*, 2723–2796.
- Norman, D.; Live, D.; Sastry, M.; Lipman, R.; Hingerty, B. E.; et al. NMR and computational characterization of mitomycin cross-linked to adjacent deoxyguanosines in the minor groove of the d(TACGTA)–d(TACGTA) duplex. *Biochemistry* **1990**, *29*, 2861–2875.
- Taatjes, D. J.; Fenick, D. J.; Koch, T. H. Nuclear targeting and nuclear retention of anthracycline–formaldehyde conjugates implicates DNA covalent binding in the cytotoxic mechanism of anthracyclines. *Chem. Res. Toxicol.* **1999**, *12*, 588–596.
- Cogan, P. S.; Koch, T. H. Rational design and synthesis of androgen receptor targeted non-steroidal anti-androgen ligands for the tumor specific delivery of a doxorubicin–formaldehyde conjugate. *J. Med. Chem.* **2003**, *46*, 5258–5270.
- Cogan, P. S.; Koch, T. H. Studies of targeting and intracellular trafficking of an anti-androgen-doxorubicin-formaldehyde conjugate in PC-3 prostate cancer cells bearing androgen receptor-GFP chimera. *J. Med. Chem.*, submitted.
- Burke, P. J.; Koch, T. H. Design, synthesis, and biological evaluation of doxorubicin–formaldehyde conjugates targeted to breast cancer cells. *J. Med. Chem.* **2004**, *47*, 1193–1206.
- Burke, P. J.; Kalet, B. T.; Koch, T. H. Antiestrogen binding site (AEBS) and estrogen receptor (ER) mediate uptake and distribution of 4-hydroxytamoxifen-targeted doxorubicin–formaldehyde conjugate in breast cancer cells. *J. Med. Chem.*, submitted.
- Burkhart, D. J.; Kalet, B. T.; Koch, T. H. Doxorubicin–formaldehyde conjugates targeting alpha-v beta-3 integrin. *Mol. Cancer Ther.* **2004**, *3*, 1593–1604.
- Cutts, S. M.; Rephaeli, A.; Nudelman, A.; Hmelnsky, I.; Phillips, D. R. Molecular basis for the synergistic interaction of adriamycin with the formaldehyde-releasing prodrug pivaloyloxymethyl butyrate (AN-9). *Cancer Res.* **2001**, *61*, 8194–8202.
- Dernell, W. S.; Powers, B. E.; Taatjes, D. J.; Cogan, P.; Gaudiano, G.; et al. Evaluation of the epidoxorubicin–formaldehyde conjugate, epidoxoform, in a mouse mammary carcinoma model. *Cancer Invest.* **2002**, *20*, 712–723.